



Title	Growth of nanographite on Pt(111) and its edge state
Author(s)	Entani, Shiro; Ikeda, Susumu; Kiguchi, Manabu; Saiki, Koichiro; Yoshikawa, Genki; Nakai, Ikuyo; Kondoh, Hiroshi; Ohta, Toshiaki
Citation	Applied Physics Letters, 88(15), 153126 https://doi.org/10.1063/1.2194867
Issue Date	2006-04-10
Doc URL	http://hdl.handle.net/2115/29768
Rights	Copyright © 2006 American Institute of Physics
Type	article
File Information	APL88-15.pdf



[Instructions for use](#)

Growth of nanographite on Pt(111) and its edge state

Shiro Entani, Susumu Ikeda, Manabu Kiguchi, and Koichiro Saiki^{a)}
Department of Complexity Science and Engineering, The University of Tokyo, 5-1-5 Kashiwanoha, Kashiwa-shi, Chiba 277-8561, Japan

Genki Yoshikawa, Ikuyo Nakai, Hiroshi Kondoh, and Toshiaki Ohta
Department of Chemistry, The University of Tokyo, 7-3-1 Hongo, Bunkyo-ku, Tokyo 113-0033, Japan

(Received 24 November 2005; accepted 2 March 2006; published online 14 April 2006)

The nanographite grains, the diameter of which was around 5 nm, were formed on Pt(111) by exposing the Pt(111) substrate to benzene gas at room temperature and annealing it up to 850 K. The increase of relative number of edge atoms enabled the observation of edge-derived electronic states. The measurement of ultraviolet photoelectron spectroscopy and near edge x-ray absorption fine structure on the nanographite revealed the appearance of the edge state located at the Fermi level.
 © 2006 American Institute of Physics. [DOI: 10.1063/1.2194867]

The nature of graphite edges has attracted considerable attention for its peculiar electronic states. In the graphitic structure, there are two types of edges: a zigzag edge and an armchair edge. Theoretical studies of single layer graphite ribbons show that the zigzag edge has a localized edge state at the Fermi level (E_F), while the armchair edge has no such state.¹ First principles calculations show that magnetic instability may occur due to a Fermi surface instability in the zigzag edge state.² Experimentally, the peculiar electronic structures, arising from this “edge state,” were observed by means of scanning tunneling spectroscopy (STS) measurements.^{3–6} In these studies, the edge state appearing only at the peripheral region of the graphite was observed by local probe techniques. The electronic structure of the greater part of the sample, on the other hand, is that of the bulk graphite. For a practical use it is necessary to enhance the contribution of the edge in the graphitic structure. In the past works artificial synthesis of the graphite edges was examined.^{7,8} However, the electronic structure characteristic of the edge state has not been observed yet. If the nanometer scale graphite grains could be fabricated, the nature inherent in the edge states would appear on the macroscopic scale. In the present work we tried to synthesize the nanometer scale graphite (nanographite) grains to aim at realizing the appearance of zigzag edge state on the macroscopic scale.

The experiments were performed in a custom-designed ultrahigh-vacuum (UHV) system with a base pressure of 10^{-7} Pa. A mechanically and electrochemically polished Pt(111) substrate was cleaned by repeated cycles of Ar⁺ sputtering and annealing at 1300 K. The specimen of nanographite film was prepared by exposing the Pt(111) substrate to a 200 L (1 L = 1×10^{-6} torr sec) benzene gas at room temperature (RT) and annealing it up to 850 K for 30 min. After the growth, Auger electron spectrum (AES) and ultraviolet photoelectron spectrum (UPS) were measured with a hemispherical energy analyzer (SPECS, PHOIBOS-100). C *K*-edge near edge x-ray absorption fine structure (NEXAFS) was measured at the BL-7A of the Photon Factory in the Institute of Material Structure Science (Tsukuba, Japan). The partial electron yield method was adopted to obtain C *K*-edge NEXAFS.⁹ All the spectroscopic measurements were done in

ultrahigh vacuum without the grown specimen exposed to the atmosphere. The surface morphology was observed by a scanning tunneling microscope (STM) in the atmosphere.

Figure 1(a) shows a STM image of the nanographite film. As shown in the inset of Fig. 1(a), the film grown at RT consists of plenty of grains whose diameters were approximately 5 nm. When the Pt substrate was exposed to benzene gas at elevated temperatures, the grain size increased with the increasing substrate temperature, as shown in Fig. 1(c). We defined the specimen fabricated at RT as the nanographite film and investigated the electronic structure of the film by spectroscopic measurements. In order to characterize the nanographite film through comparison with the graphite of the same thickness, a single layer graphite (graphene) film was prepared by chemical vapor deposition.¹⁰ Figure 1(b) shows a STM image of the graphene film. A large flat area was observed in the graphene film in contrast with the image

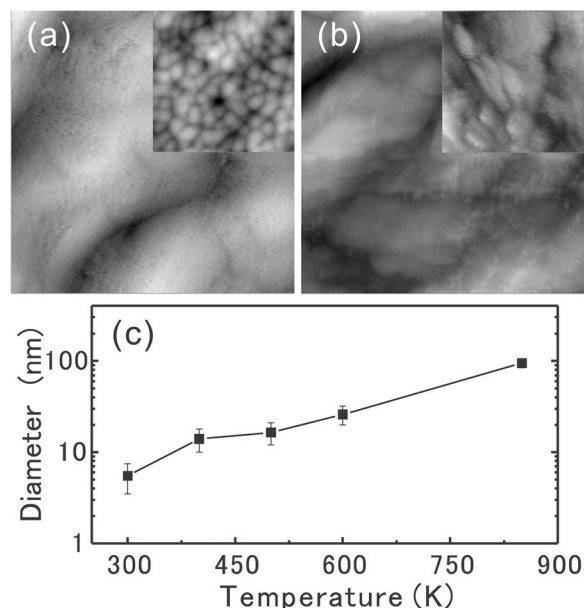


FIG. 1. (a) A STM image of a nanographite film ($1.5 \times 1.5 \mu\text{m}^2$, $T=300$ K, in air). The inset shows $50 \times 50 \text{ nm}^2$ STM image. (b) A STM image of a graphene film prepared by the method of Ref. 10 ($1.5 \times 1.5 \mu\text{m}^2$, $T=300$ K, in air). (c) Temperature dependence of the mean diameter of the graphite grains.

^{a)}Electronic mail: saiki@k.u-tokyo.ac.jp

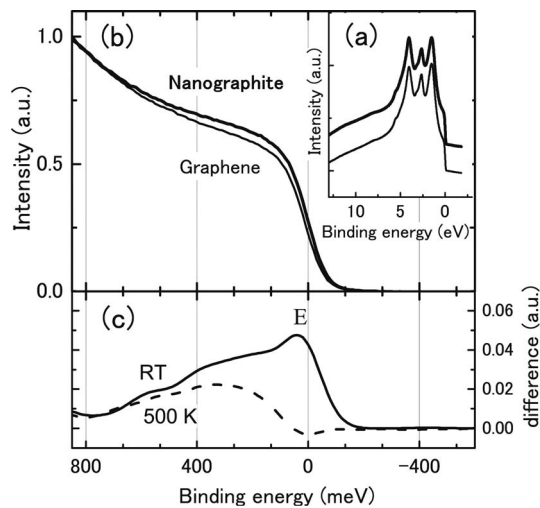


FIG. 2. (a) UPS of the nanographite and graphene films measured with a He I (21.2 eV) source. (b) UPS spectra of the nanographite and graphene films around E_F . (c) Difference spectrum between the nanographite and graphene films (solid line) and that between the graphite grain grown at 500 K and graphene films (dashed line).

of Fig. 1(a). Judging from the intensity of carbon signal in their Auger electron spectra, the surface coverage was around 0.9 in both films.

As we could prepare the nanographite film, the electronic structure was investigated *in situ* by UPS and NEXAFS. Figure 2(a) shows the UPS spectrum of the nanographite and the graphene films measured with a He I (21.2 eV) source. In these spectra, there appeared four platinum-derived states at 0.14, 1.5, 2.6, and 4.0 eV.¹¹ The UPS spectra in the region with binding energies larger than 0.8 eV were almost the same between the nanographite and graphene films. In the narrower energy range spectrum [Fig. 2(b)], however, there is a difference near the E_F . In order to see the difference, the graphene spectrum was subtracted from the nanographite spectrum [solid line in Fig. 2(c)]. It is clearly seen that an electronic state E is formed in the nanographite spectrum grown at RT. In addition, the difference was found to decrease for the graphite grains grown at 500 K. In the nanographite grains, the zigzag edge and the armchair edge would be intermingled. The theoretical studies predict that the zigzag edge state causes the electronic states around the E_F , which could be distinguished from that of bulk graphite.¹ On the contrary, the armchair edge state would be smeared in that of bulk graphite. Thus it is likely that the electronic state (E) in the difference spectrum is considered to originate from the occupied zigzag edge state.

Figure 3(a) shows the NEXAFS spectrum of the nanographite film. Three main features are observed in the spectrum: a shoulder at 283.8 eV ($p1$), a sharp peak at 285.1 eV ($p2$), and another sharp peak at 287.5 eV ($p3$). Two intense peaks ($p2$ and $p3$) are assigned to the $C1s$ -to- π^* ($C=C$) transition and to the $C1s$ -to- σ^* ($C-H$) transition, respectively.¹² In contrast, the small peak at 283.8 eV has not been reported yet. The position of the E_F can be estimated from the binding energy of $C1s$ x-ray photoelectron spectroscopy (XPS) spectra (not shown here) and it is located at 284.0 eV, a little higher than the peak ($p1$). The transition energy observed in the NEXAFS spectrum is determined by final state effect, not the ground state properties. It depends on the intramolecular screening, i.e., self-screening of the

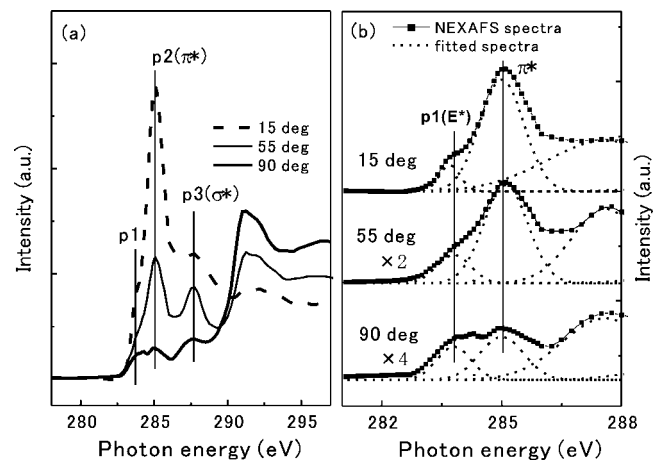


FIG. 3. (a) Polarization dependence of the C K -edge NEXAFS spectra of the nanographite grains. (b) Narrower energy range NEXAFS spectra.

core hole by the excited electron. Therefore, it is not unreasonable that the empty state can be observed below the E_F , which is determined by XPS.¹³ Thus an empty state (E^*) is considered to be formed at the energy close to E_F . Since the C K -edge NEXAFS observes the empty states arising from the carbon orbitals, the observed E^* state reflects the electronic structure of the nanographite. The NEXAFS and UPS results indicated that we are dealing with a broad surface state which is centered at the Fermi level and is partially occupied. It can be considered that these states (E and E^*) originate from the edge states appearing at the zigzag edge of graphite. Finally, the intensity ratio of the $p1$ peak to the π^* peak is estimated to be 0.18, which is close to 0.20 expected for the number ratio of peripheral carbon atoms to the interior carbon atoms in the round-shaped nanographite with the diameter of 5 nm.

The advantage of NEXAFS is the possibility to discuss the geometry of the final state. We discuss the edge state (E^*) from the polarization dependent NEXAFS spectra, as shown in Fig. 3(b). In the present case, the NEXAFS intensity is written as $I = PI^{\parallel} + (1-P)I^{\perp}$, using polarization factor P , the intensities associated with parallel and perpendicular components of the incident x ray, I^{\parallel} and I^{\perp} , described below.

$$I^{\parallel} = \frac{1}{3} \left[1 + \frac{1}{2} (3 \cos^2 \theta - 1) (3 \cos^2 \alpha - 1) \right], \quad (1)$$

$$I^{\perp} = \frac{1}{2} \sin^2 \alpha,$$

where θ is the x-ray incidence angle from the surface and α is the polar angle of the molecular orbital. The NEXAFS spectra of the π^* peaks and E^* peaks were fitted with the above equations,¹³ and the mean inclination angles of π^* and E^* orbitals were estimated to be 22° and 44° from the surface normal, respectively. Judging from the inclination angle of the π^* state, the interior of nanographite grains is not completely parallel to the substrate, which would have been expected for a flat graphite flake. The larger inclination angle of the E^* state suggests that the peripheral region of the nanographite grains is much more tilted from the surface parallel so that the shape of the nanographite grains is like a pressed dome, which can be observed by the STM images. Theoretical investigations reported that the lattice distortion is in-

duced by an electron-phonon interaction in the nanographene ribbons.¹⁴ The lattice distortion would cause the deformation of the nanographite grains due to disadvantage of the flatness.

In conclusion, we have succeeded in preparing the nanographite films, the diameter of which was as small as 5 nm. The electronic structure characteristic of the edge state was observed by a conventional spectroscopic method, which could be realized by increasing the component of edge states. The present result opens a way to reveal the intriguing property such as magnetism originating from the zigzag edge states of graphite.

This work was supported by a Grant-in-Aid from the Ministry of Education, Culture, Sports, Science and Technology of Japan (14GS0207). The NEXAFS measurement was performed under the approval of the Photon Factory Program Advisory Committee (proposal No. 2003G259).

¹K. Nakada, M. Fujita, G. Dresselhaus, and M. S. Dresselhaus, *Phys. Rev.*

B **54**, 17954 (1996).

²S. Okada and A. Oshima, *Phys. Rev. Lett.* **87**, 146803 (2001).

³Z. Klusek, Z. Waqar, E. A. Denisov, T. N. Kompaniets, I. V. Makareno, A. N. Titkov, and A. S. Bhatti, *Appl. Surf. Sci.* **161**, 508 (2000).

⁴Z. Klusek, *Vacuum* **63**, 139 (2001).

⁵Y. Niimi, T. Matsui, H. Kambara, K. Tagami, M. Tsukada, and H. Fukuyama, *Appl. Surf. Sci.* **241**, 43 (2005).

⁶Y. Kobayashi, K. Fukui, T. Enoki, K. Kusakabe, and Y. Kaburagi, *Phys. Rev. B* **71**, 193406 (2005).

⁷M. Terai, N. Hasegawa, M. Okusawa, S. Otani, and C. Oshima, *Appl. Surf. Sci.* **130–132**, 876 (1998).

⁸T. Tanaka, A. Tajima, R. Moriizumi, M. Hosoda, R. Ohno, E. Rokuta, C. Oshima, and S. Otani, *Solid State Commun.* **123**, 33 (2002).

⁹K. Amemiya, H. Kondoh, T. Yokoyama, and T. Ohta, *J. Electron Spectrosc. Relat. Phenom.* **124**, 151 (2002).

¹⁰H. Zi-pu, D. F. Ogletree, M. A. Van Hove, and G. A. Somorjai, *Surf. Sci.* **180**, 433 (1987).

¹¹S. F. Lin, D. T. Pierce, and W. E. Spicer, *Phys. Rev. B* **4**, 326 (1971).

¹²J. Kikuma, K. Yoneyama, M. Nomura, T. Konishi, T. Hashimoto, R. Mitsumoto, Y. Ohuchi, and K. Seki, *J. Electron Spectrosc. Relat. Phenom.* **88–91**, 919 (1998).

¹³J. Stöhr, *NEXAFS Spectroscopy* (Springer, New York, 1991).

¹⁴M. Fujita, M. Igami, and K. Nakada, *J. Phys. Soc. Jpn.* **66**, 1864 (1997).